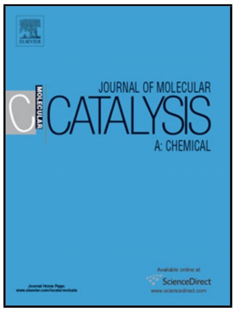

Title: Gas-phase epoxidation of propylene by molecular oxygen over Ag-$CuCl_2$/$BaCO_3$ catalyst with low $CuCl_2$ doping: Catalytic performance, deactivation and regeneration

Author: Qing Zhang Guangtao Chai Yanglong Guo Wangcheng Zhan Yun Guo Li Wang Yunsong Wang Guanzhong Lu

PII: S1381-1169(16)30343-0
DOI: http://dx.doi.org/doi:10.1016/j.molcata.2016.08.019
Reference: MOLCAA 10006

To appear in: *Journal of Molecular Catalysis A: Chemical*

Received date: 14-7-2016
Revised date: 13-8-2016
Accepted date: 16-8-2016

Please cite this article as: Qing Zhang, Guangtao Chai, Yanglong Guo, Wangcheng Zhan, Yun Guo, Li Wang, Yunsong Wang, Guanzhong Lu, Gas-phase epoxidation of propylene by molecular oxygen over Ag-CuCl2/BaCO3 catalyst with low CuCl2 doping: Catalytic performance, deactivation and regeneration, Journal of Molecular Catalysis A: Chemical http://dx.doi.org/10.1016/j.molcata.2016.08.019

<AT>Gas-phase epoxidation of propylene by molecular oxygen over Ag-CuCl$_2$/BaCO$_3$ catalyst with low CuCl$_2$ doping: catalytic performance, deactivation and regeneration

<AU>Qing Zhang, Guangtao Chai, Yanglong Guo*
##Email##ylguo@ecust.edu.cn##/Email##, Wangcheng Zhan, Yun Guo, Li Wang, Yunsong Wang, Guanzhong Lu* ##Email##gzhlu@ecust.edu.cn##/Email##
<AFF>Key Laboratory for Advanced Materials, Research Institute of Industrial Catalysis, School of Chemistry and Molecular Engineering, East China University of Science and Technology, Shanghai 200237, P R China
<PA>Fax: +86 21 64252923.

<ABS-Head><ABS-HEAD>Graphical abstract
<ABS-P>
<ABS-P><xps:span class="xps_Image">fx1</xps:span>

<ABS-HEAD>Highlights►

<remove picture pageno 1>Ag-CuCl$_2$/BaCO$_3$ catalyst was prepared by reduction-deposition-impregnation method.

<remove picture pageno 1>Ag-CuCl$_2$/BaCO$_3$ catalyst with low CuCl$_2$ doping exhibits better catalytic performance.

<remove picture pageno 1>Epoxidation of propylene over Ag-CuCl$_2$/BaCO$_3$ catalyst follows Rideal-Eley mechanism.

<remove picture pageno 1>Molecular oxygen species benefit epoxidation of propylene to propylene oxide.► ►Ag-based catalyst is deactivated by coke deposition and can be entirely regenerated.

<ABS-HEAD>ABSTRACT

<ABS-P>Ag-MCl$_x$/BaCO$_3$ catalysts with different chloride promoters, prepared by reduction-deposition-impregnation method, were investigated for gas-phase epoxidation of propylene to propylene oxide (PO) by molecular oxygen. Ag-CuCl$_2$/BaCO$_3$ catalyst with 360 ppm of Cu and 400 ppm of Cl exhibits the best initial catalytic performance, in which PO selectivity of 71.2% and propylene conversion of 1.3% are achieved, but only PO selectivity of 13.9% is obtained at propylene conversion of 3.2% after reaction for 500 min. The catalytic reaction mechanism over Ag-CuCl$_2$/BaCO$_3$ catalyst follows Rideal-Eley mechanism, in which propylene in the gas phase reacts with molecular oxygen species adsorbed on the surface of Ag at the interface in close contact with CuCl$_2$ to produce PO, and with atomic oxygen species adsorbed on the surface of Ag nanoparticles to produce CO$_2$ and H$_2$O. One oxygen atom of molecular oxygen species reacts with propylene to form a PO molecule, and the left insufficient oxygen atoms react with propylene to produce oxygen-containing intermediates

and then to form coke deposition which covers the active sites and thus results in the catalyst deactivation. The deactivated Ag-$CuCl_2/BaCO_3$ catalyst can be completely regenerated by combustion of coke deposition and then impregnation with appropriate amount of Cl.

<KWD>Keywords: Epoxidation of propylene; Propylene oxide; Molecular oxygen; Ag-based catalyst; $CuCl_2$ doping.

<H1>1. Introduction

Propylene oxide (PO) is a versatile synthetic intermediate widely used for production of propylene glycols, polyether polyols, polyurethane, surfactants and other commercial products. PO is produced mainly by the chlorohydrin process, the Halcon process and the hydroperoxide process. However, the chlorohydrin process is environmentally unfriendly, the Halcon process generates the equimolar coproducts which values depend on their demands in the market [1] and the commercialization of the hydroperoxide process is hindered by the expense and transport of H_2O_2 and the commercial installation [2-3]. Though Au-based catalysts can produce PO with high selectivity by the in-situ production of H_2O_2 from H_2-O_2 mixture [4-11], H_2 must be used as a sacrificial coreactant and its efficiency is usually low. As oxygen is a cheap and green oxidant, gas-phase epoxidation of propylene by molecular oxygen is the most ideal reaction process with high atomic economy, however, remains a great challenge for researchers to attain higher PO selectivity.

Epoxidation of ethylene by molecular oxygen over Ag-based catalysts has been widely used in the industrial production of ethylene oxide (EO) with the selectivity of 83-95 % for many years [12-14], whereas, epoxidation of propylene by molecular oxygen over Ag-based catalysts is still under investigation, in which unpromoted Ag catalysts are inefficient for PO formation with PO selectivity of below 10 % [15-18]. Al_2O_3 is widely used as the support of Ag-based catalysts for epoxidation of ethylene by molecular oxygen, however, is not an efficient support for epoxidation of propylene by molecular oxygen, because high surface area and the acidity of Al_2O_3 support easily lead to the complete combustion of propylene and PO [17]. Various promoters, such as K, MoO_3, Y_2O_3 and Cu, have been investigated to improve

PO selectivity [19-23]. In the industrial production process of EO, EO selectivity can be improved by addition of chlorohydrocarbon in the feed gas, which indicates that Cl is benefit for EO formation. Cl-promoted Ag catalysts were prepared to improve EO selectivity and Cl effect was investigated [24-26]. In view of the similarity between ethylene and propylene, both addition of chlorohydrocarbon in the feed gas [27] and modification of various chlorides, such as NaCl, $BaCl_2$, CsCl and CuCl, enhanced PO selectivity for epoxidation of propylene by molecular oxygen [28-31]. The promotion of Cl was also investigated for epoxidation of butadiene [32]. Cl was thought to work best among all halogen elements for its electronic effect [33]. Cu catalyst was more efficient for epoxide formation than Ag catalyst, because oxygen species adsorbed on Cu surface tended to attack C=C bond to form epoxide rather than strip allylic hydrogen leading to combustion of propylene [34-36]. Cu-based catalysts modified with VO_x, RuO_x and MnO_x exhibited better catalytic performance for epoxidation of propylene [37-39]. The low valance state of Cu was thought to be more effective for epoxidation of propylene [40-42].

The reaction mechanism of epoxidation of propylene by molecular oxygen over Ag-based catalysts has been discussed for many years. Because oxygen species adsorbed on the surface of Ag catalyst are nucleophilic (i. e. high-basicity oxygen) rather than electrophilic (i. e. low-basicity oxygen) [36], the markedly basic character of oxygen species leads to the stripping of allylic hydrogen atoms and then the complete combustion of propylene to CO_2, which results in worse catalytic performance.

$BaCO_3$ with low surface area and medium basicity is chosen as the support of Ag-based catalysts for gas-phase epoxidation of propylene by molecular oxygen, in which 12.5 % of propylene conversion and 36.9 % of PO selectivity are achieved [43]. In this work, Ag-MCl_x/$BaCO_3$ catalysts with different chloride promoters, prepared by the reduction-deposition-impregnation method, were investigated for gas-phase epoxidation of propylene by molecular oxygen, in which effects of the chloride promoters, $CuCl_2$ loading, the calcination temperature, the reaction temperature and gas hourly space velocity were studied. The aim of this work was to clarify oxygen species and active sites responsible for PO formation over Ag-$CuCl_2$/$BaCO_3$ catalyst, and the catalytic reaction mechanism for epoxidation of propylene by molecular oxygen was proposed. Moreover, the catalyst stability, the deactivation mechanism and the regeneration way of Ag-$CuCl_2$/$BaCO_3$ catalyst were also investigated.

<H1>2. Experimental

<H2>2.1. Preparation of catalysts

Ag/$BaCO_3$ catalyst was prepared by the reduction-deposition method as follows [43]: 8.0 g of $BaCO_3$ support was firstly immersed into the aqueous solution of ethylene diamine for 12 h and then dried at 60 °C under vacuum for 4.5 h. After that, 2.0 g of formaldehyde (HCHO) was dissolved in 40.0 mL of deionized water as the reductant, into which the dried amine-pretreated $BaCO_3$ support was added to form a slurry in the ice-water bath at 10 ^{o}C. After stirring for 20 min, 0.6 g of $AgNO_3$ dissolved in 40.0 mL of deionized water was added dropwise into the above slurry, then the solid was filtered and washed with deionized water and ethanol for several times. The solid was dried overnight at room temperature and then calcined in N_2 atmosphere at 250 ^{o}C for 4 h. Ag-$CuCl_2$/$BaCO_3$ catalysts were prepared by the incipient impregnation of the dried Ag/$BaCO_3$ catalyst without calcination with the aqueous solution of $CuCl_2$ for 12 h, dried at 60 °C and then calcined in N_2 atmosphere at 250 ^{o}C for 4 h. The similar procedures were used to prepare Ag-MCl_x/$BaCO_3$ catalysts modified with other promoters (NH_4Cl, NaCl, KCl, $CaCl_2$ and $FeCl_3$), except for Ag-CuCl/$BaCO_3$ catalyst prepared by the ball-milling treatment of the dried Ag/$BaCO_3$ catalyst without calcination with CuCl powder at 800 rpm for 10 h and then calcined in N_2 atmosphere at 250 ^{o}C for 4 h. $CuCl_2$/$BaCO_3$ catalyst was prepared by the incipient impregnation of $BaCO_3$ support with the aqueous solution of $CuCl_2$ for 12 h, dried at 60 °C and then calcined in N_2 atmosphere at 250 ^{o}C for 4 h.

<H2>2.2. Epoxidation of propylene

Epoxidation of propylene was carried out in a fixed-bed quartz reactor under the reaction conditions of 0.6 g catalyst, 200 °C, 0.1 MPa and GHSV of 3000 h^{-1}. The feed gas consisted of 20 % of propylene, 10 % of O_2 and balance N_2. Reaction products were analyzed by two on-line gas chromatographs equipped with a two packed columns (G.D.X-401 and Porapak Q) with FID and TCD detectors. All lines between the reactor exit and the gas chromatographs were heated to 120 °C in order to prevent condensation of products. PO selectivity and propylene conversion were calculated on a carbon balance basis.

<H2>2.3. Characterization of catalysts

Elemental analysis was done by inductively coupled-plasma atomic emission spectroscopy (ICP-AES) using a TJA IRIS ADVANTAG 1000 instrument.

XRD patterns were performed on a Bruker AXS D8 Focus diffractometer operated at 40 kV, 40 mA (Cu Kα radiation, $\lambda = 0.15406$ nm).

XPS spectra were recorded on a Thermo ESCALAB 250 spectrometer with a monochromatized AlKα X-ray source (1486.6 eV) and a passing energy of 20 eV. C1s (binding energy of 284.6 eV) of adventitious carbon was used as the reference.

H_2-TPR experiments were carried out in a conventional flow system equipped with a TCD detector. 500 mg samples of 40-60 mesh were loaded in a quartz reactor and then heated programmedly from 25 °C to 350 °C at a heating rate of 10 $^{o}C\cdot min^{-1}$ in a gas flow of H_2-N_2 (5 vol. % H_2) of 45 $mL\cdot min^{-1}$.

TEM images were recorded on a JEM-2100 transmission electron microscope. The sample was ultrasonically suspended in the ethanol solvent, and one drop of this slurry was deposited on a molybdenum grid. The liquid phase was evaporated before the grid was loaded into the microscope.

Temperature programmed desorption of O_2 (O_2-TPD) and C_3H_6 (C_3H_6-TPD), temperature programmed oxidation of O_2 (O_2-TPO) and temperature programmed surface reaction of C_3H_6 (C_3H_6-TPSR) were carried out on a Micromeritics AutoChem 2920 Ⅱ chemisorption analyzer with a Hiden HPR 20 mass spectrometer. For O_2-TPD and C_3H_6-TPD, 500 mg samples of 40-60 mesh were loaded in a quartz reactor and pretreated in a He flow of 30 $mL\cdot min^{-1}$ at 250 ^oC for 0.5 h. After it was cooled down to room temperature, a gas flow of O_2-He (3 vol. % O_2) or a gas flow of C_3H_6-Ar (1 vol. % C_3H_6) of 20 $mL\cdot min^{-1}$ was introduced into the reactor, the reactor temperature was raised to 200 ^oC at a rate of 10 $^oC\cdot min^{-1}$ and was kept at 200 ^oC for 0.5 h, then cooled down to room temperature. After that, a He flow of 20 $mL\cdot min^{-1}$ was switched. When the baseline was stable, the reactor temperature was raised to 600 ^oC at a heating rate of 10 $^oC\cdot min^{-1}$. The MS signals of O_2 (m/e = 32) or C_3H_6 (m/e = 41) were recorded by the mass spectrometer. For C_3H_6-TPSR, a gas flow of C_3H_6-Ar (20 vol. % C_3H_6) of 20 $mL\cdot min^{-1}$ was introduced into the reactor after the pretreatment with a gas flow of O_2-He (3 vol. % O_2) of 20 $mL\cdot min^{-1}$ similar to O_2-TPD. The MS signals of PO (m/e = 58) and CO_2 (m/e = 44) were recorded by the mass spectrometer. For O_2-TPO experiment, a gas flow of O_2-He (3 vol. % O_2) of 10 $mL\cdot min^{-1}$ was introduced into the quartz reactor loaded with 500 mg samples of 40-60 mesh. The reactor temperature was raised to 450 ^oC at a heating rate of 10 $mL\cdot min^{-1}$. The MS signals of O_2 (m/e = 32), CO_2 (m/e = 44) and H_2O (m/e = 18) were recorded by the mass spectrometer.

<H1>3. Results and discussion

<H2>3.1. Catalytic performance of Ag-MCl_x/$BaCO_3$ catalysts

Table 1 shows effect of the chloride promoters on the catalytic performance of Ag-MCl_x/$BaCO_3$ catalysts for gas-phase epoxidation of propylene by molecular oxygen. As shown in Table 1, Ag/$BaCO_3$ catalyst without promoter exhibited high propylene conversion of 12.5 % and medium PO selectivity of 36.9 %, in which CO_2 was by-product with the selectivity of 63.1 %. The modification of Ag/$BaCO_3$ by the chloride promoters shown in Table 1 all decreased propylene conversion probably because the introduction of chlorides decreased the number of bare Ag sites [33]. The modification of NH_4Cl, NaCl, $CaCl_2$ or $FeCl_3$ decreased propylene conversion significantly to < 1 %, the modification of KCl or $CuCl_2$

exhibited propylene conversion of 1-2 %, and relatively high propylene conversion of 5.2 % was achieved over Ag-CuCl/$BaCO_3$ catalyst. The modification of the chlorides did not exert positive effects on PO selectivity except for Ag-$CuCl_2$/$BaCO_3$ catalyst. PO selectivity reached 71.2 % at propylene conversion of 1.3 % over Ag-$CuCl_2$/$BaCO_3$ catalyst. Over all catalysts modified with the chlorides, besides the main by-product of CO_2, there was another by-product of acrolein (PA) with the selectivity of below 1% which could almost be ignored. Therefore Ag-$CuCl_2$/$BaCO_3$ catalyst exhibited better PO selectivity than Ag/$BaCO_3$ catalyst despite a decrease in propylene conversion for epoxidation of propylene by molecular oxygen, which would be mainly investigated in detail.

<H2>3.2. Effect of $CuCl_2$ loading

To gain further insights into the synergistic effect between $CuCl_2$ and Ag, effect of $CuCl_2$ loading on the catalytic performance of Ag-$CuCl_2$/$BaCO_3$ catalyst was investigated for epoxidation of propylene by molecular oxygen, which is shown in Table 2. Ag loadings of all Ag-containing catalysts were at the similar values of 4.3 wt. % measured by ICP-AES. As shown in Table 2, both propylene conversion and PO selectivity were much lower and PA selectivity was a little higher over $CuCl_2$/$BaCO_3$ catalysts than the corresponding Ag-$CuCl_2$/$BaCO_3$ catalysts, which indicated that only the combination of Ag and $CuCl_2$ was effective for PO formation probably due to the significant synergistic effect between them. Moreover, with an increase in $CuCl_2$ loading from 180 ppm of Cu and 200 ppm of Cl up to 720 ppm of Cu and 800 ppm of Cl over Ag-$CuCl_2$/$BaCO_3$ catalyst, propylene conversion significantly decreased from 2.9 % to 0.3 %, because Cl could cover and then poison the active sites of Ag at high levels [33]. As for PO selectivity, Ag-$CuCl_2$/$BaCO_3$ catalyst with the promoter of 180 ppm of Cu and 200 ppm of Cl obtained PO selectivity of only 15.5 %, even lower than Ag/$BaCO_3$ catalyst. However, it was interesting that Ag-$CuCl_2$/$BaCO_3$ catalyst with the promoter of 360 ppm of Cu and 400 ppm of Cl obtained PO selectivity of 71.2 %. With further increasing $CuCl_2$ loading, PO selectivity decreased and CO_2 selectivity increased. Turnover frequency (TOF) values of PO formation based on Ag atoms on the catalyst surface, i. e. moles of PO produced per mole of surface Ag per second, were calculated [37, 44]. Compared with Ag/$BaCO_3$ catalyst, TOF values of PO formation of Ag-$CuCl_2$/$BaCO_3$ catalysts decreased largely due to much lower propylene conversion. Among

Ag-$CuCl_2$/$BaCO_3$ catalysts with different $CuCl_2$ loadings, Ag-$CuCl_2$/$BaCO_3$ catalyst with 360 ppm of Cu and 400 ppm of Cl achieved the highest TOF value of $2.0*10^{-4}$ s^{-1} of PO formation. Therefore only the appropriate modification amount of $CuCl_2$ promoter of Ag-$CuCl_2$/$BaCO_3$ catalyst can improve PO selectivity for epoxidation of propylene by molecular oxygen.

<H2>3.3. Effect of reaction conditions

Fig. 1 shows effect of the reaction temperature on the catalytic performance of Ag/$BaCO_3$ catalyst and Ag-$CuCl_2$/$BaCO_3$ catalyst with 360 ppm of Cu and 400 ppm of Cl. Over Ag/$BaCO_3$ catalyst, with increasing the reaction temperature, PO selectivity decreased gradually from 40.3 % at the reaction temperature of 80 ^{o}C to 36.9 % at the reaction temperature of 200 ^{o}C, but propylene conversion increased obviously from 0.4 % at the reaction temperature of 80 ^{o}C to 12.5 % at the reaction temperature of 200 ^{o}C. However, over Ag-$CuCl_2$/$BaCO_3$ catalyst, with an increase in the reaction temperature, PO selectivity decreased significantly from nearly 100 % at the reaction temperature of 80 ^{o}C to 71.2 % at the reaction temperature of 200 ^{o}C and only 47.5 % at the reaction temperature of 240 ^{o}C, but propylene conversion increased gradually, in which propylene conversions were 0.2 %, 1.3 % and 5.5 %, respectively, at the reaction temperatures of 80 ^{o}C, 200 ^{o}C and 240 ^{o}C. As shown in Fig. 2, good linear relations between the logarithm of the reaction rate of epoxidation of propylene and the reciprocal of the reaction temperature were obtained over Ag/$BaCO_3$ and Ag-$CuCl_2$/$BaCO_3$ catalysts, in which the apparent activation energies were 40.7 $KJ \cdot mol^{-1}$ and 23.0 $KJ \cdot mol^{-1}$, respectively. The decrease in the apparent activation energy after modification of $CuCl_2$ may imply the change of the reaction pathway and the product distribution, which agrees well with the catalytic performance of Ag/$BaCO_3$ and Ag-$CuCl_2$/$BaCO_3$ catalysts shown in Table 2.

Fig. 3 shows effect of gas hourly space velocity (GHSV) on the catalytic performance of Ag-$CuCl_2$/$BaCO_3$ catalyst with 360 ppm of Cu and 400 ppm of Cl. A decrease in GHSV from 6000 h^{-1} to 1500 h^{-1} increased propylene conversion from 0.4% to 2.0% and PO selectivity from 70.1% to 75.4 %. Over Ag-$CuCl_2$/$BaCO_3$ catalyst, PO selectivity of 75.4 % and propylene conversion of 2.0 % at GHSV of 1500 h^{-1} were better than those at GHSV of 3000 h^{-1} in which PO selectivity of 71.2 % and propylene conversion of 1.3 % were obtained.

<H2>3.4. Characterization of Ag-$CuCl_2$/$BaCO_3$ catalyst

To gain information about the valence states of Ag, Cu and Cl, XPS spectra of Ag-$CuCl_2$/$BaCO_3$ catalysts with different $CuCl_2$ loadings were performed. As shown in Fig. 4A, the satellite peak at 942 eV was not detected over all Ag-$CuCl_2$/$BaCO_3$ catalysts, which implied the absence of Cu^{2+} species. The binding energies of Cu $2p_{3/2}$ and Cu $2p_{1/2}$ of all catalysts were 933.1-934.8 eV and 952.8-954.5 eV respectively, which indicated the valence state of Cu was between +1 and +2, and there existed strong interaction between $CuCl_2$ and Ag. The binding energies of Cu $2p_{3/2}$ and Cu $2p_{1/2}$ of Ag-$CuCl_2$/$BaCO_3$ catalyst with 360 ppm of Cu and 400 ppm of Cl were the lowest, 933.1 eV and 952.8 eV respectively, which indicated that there existed the strongest interaction between Cu and Ag and thus was beneficial for PO formation. Fig. 4B shows Cl 2p XPS spectra of Ag-$CuCl_2$/$BaCO_3$ catalyst, in which the binding energy was 198 eV assignable to Cl^- species. [45] The peak of Cl 2p of Ag-$CuCl_2$/$BaCO_3$ catalyst with higher $CuCl_2$ loading was not obvious because of the surface enrichment of Cu species. As shown in Fig. 4C, the binding energies of Ag $3d_{3/2}$ and Ag $3d_{5/2}$ of all Ag-$CuCl_2$/$BaCO_3$ catalysts were at the same values of 374.1 eV and 368.1 eV, respectively, corresponding to Ag^0 [46, 47], which indicated that the valence state of Ag didn't change with modification of $CuCl_2$ probably because of the low $CuCl_2$ doping. As reported in the literature, the oxidation state of Ag of Ag-Pt/Al_2O_3 catalyst didn't change due to the very low Pt loading of 500 ppm [48]. Therefore there exists the strongest interactions between Ag and Cu favorable for PO formation over Ag-$CuCl_2/BaCO_3$ catalyst with 360 ppm of Cu and 400 ppm of Cl.

Table 3 shows the surface composition of Ag-$CuCl_2/BaCO_3$ catalysts with different $CuCl_2$ loadings determined by XPS. The surface concentration of Ag of Ag/$BaCO_3$ catalyst was 12.4 atom %. Interestingly, the surface concentration of Ag of Ag-$CuCl_2/BaCO_3$ catalyst with 180 ppm of Cu and 200 ppm of Cl was 12.5 atom %, which was almost the same as that of Ag/$BaCO_3$ catalyst. This indicated that 180 ppm of Cu and 200 ppm of Cl were mainly located on the surface of $BaCO_3$ support rather than the surface of Ag nanoparticles. With further increasing $CuCl_2$ loading, the surface concentration of Ag decreased gradually, which indicated that the extra part of Cu and Cl were located on the surface of Ag nanoparticles besides a part of Cu and Cl located on the surface of $BaCO_3$ support, which agreed well with H_2-TPR results shown in Fig. S2. With increasing $CuCl_2$ loading, the ratio of Ag to Cu decreased obviously, and the surface concentration of Cu and Cl increased gradually except for the situation of Cl over Ag-$CuCl_2/BaCO_3$ catalysts with higher $CuCl_2$ loadings, in which Cl was hardly detected because of the surface enrichment of Cu and thus maybe be the reason for the surface nonstoichiometric ratio of Cu to Cl.

<H2>3.5. Catalytic reaction mechanism

<H3>3.5.1. Reaction kinetics

The reaction mechanism of epoxidation of propylene by molecular oxygen over Ag-$CuCl_2/BaCO_3$ catalyst with 360 ppm of Cu and 400 ppm of Cl was investigated for its best catalytic performance among all Ag-$CuCl_2/BaCO_3$ catalysts with different $CuCl_2$ loadings. Fig. 5 shows dependence of the reaction rates of epoxidation of C_3H_6 on the partial pressure of O_2 or the partial pressure of C_3H_6 at 200 °C. As shown in Fig. 5, the reaction orders of O_2 or C_3H_6 were 0.13 or 0.94, approximately 0 and 1, respectively, that was to say, $r_{C_3H_6} = k_{C_3H_6} \cdot {P_{C_3H_6}}^{0.94} \cdot {P_{O_2}}^{0.13} \approx k_{C_3H_6} \cdot P_{C_3H_6}$, which indicated that the reaction process followed Rideal-Eley mechanism, similar to Ag/$BaCO_3$ catalyst [43]. This also implied that the modification of $CuCl_2$ didn't change the reaction mechanism.

<H3>3.5.2. C_3H_6-TPD

A better understanding of the adsorption behavior of the reactants on the catalyst surface is crucial for gaining insight into the reaction mechanism. Fig. 6 shows C_3H_6-TPD profiles of $CuCl_2/BaCO_3$, Ag/$BaCO_3$ and Ag-$CuCl_2/BaCO_3$ catalysts. As shown in Fig. 6, only a desorption peak of C_3H_6 was observed at about -30 °C over all the three catalysts, which indicated that C_3H_6 couldn't adsorb on the surface of all the three catalysts at the reaction temperature of 200 ^{o}C and the modification of $CuCl_2$ didn't change the weak interaction between C_3H_6 and Ag surface [49].

<H3>3.5.3. O_2-TPD

Fig. 7 shows O_2-TPD profiles of Ag-$CuCl_2$/$BaCO_3$ catalysts with different $CuCl_2$ loadings. As shown in Fig. 7, the desorption peaks of O_2 were observed from 100 ^{o}C to 320 ^{o}C, which indicated that O_2 could adsorb on the catalyst surface at the reaction temperature of 200 ^{o}C and there was strong interaction between O_2 and the catalyst surface. This further confirms that the reaction process is that propylene in the gas phase reacts with oxygen species adsorbed on the catalyst surface to produce products and thus follows Rideal-Eley mechanism, which is consistent with the reaction orders shown in Fig. 5.

Oxygen chemisorption on silver surfaces has been studied in great detail over the past two decades [50-56]. Oxygen species adsorbed on silver surfaces are divided into three categories: surface chemisorbed molecular oxygen species, surface chemisorbed atomic oxygen species and subsurface or bulk-dissolved atomic oxygen species. The atomic oxygen species were considered as the active oxygen species for epoxidation of both ethylene and propylene in some literatures [13, 46, 57-58]. However, there is a different viewpoint in this work. As shown in Fig. 7, there were three types of the overlapping peaks of O_2-TPD from 50 ^{o}C to 600 ^{o}C over Ag-$CuCl_2$/$BaCO_3$ catalysts with $CuCl_2$ loadings not more than 360 ppm of Cu and 400 ppm of Cl. Based on O_2-TPD profiles of an electrolytic silver catalyst reported in the literature [52], these three peaks of O_2-TPD were attributed to desorption of three types of oxygen species from the catalyst surface. The peak of O_2-TPD at 138-150 ^{o}C was attributed to desorption of chemisorbed molecular oxygen species. The peak of O_2-TPD at 222-241 ^{o}C was attributed to desorption of chemisorbed atomic oxygen species. The peak of O_2-TPD at 359-424 ^{o}C arose from segregation and desorption of bulk-dissolved (subsurface) oxygen species.

Because the reaction temperature was 200 ^{o}C, the former two oxygen species were discussed as follows.

Over Ag/$BaCO_3$ catalyst, the desorption temperatures of molecular oxygen species and atomic oxygen species were 150 ^{o}C and 222 ^{o}C, respectively. When Ag/$BaCO_3$ catalyst was modified with 180 ppm of Cu and 200 ppm of Cl, the desorption peak of molecular oxygen species shifted to low temperature at 140 ^{o}C, and the desorption peak of the atomic oxygen species shifted to high temperature at 225 ^{o}C. When Ag/$BaCO_3$ catalyst was modified with 360 ppm of Cu and 400 ppm of Cl, the desorption temperature of molecular oxygen species also shifted to lower temperature at 138 ^{o}C, and the desorption peak of atomic oxygen species also shifted to higher temperature at 241 ^{o}C with the significantly decreased intensity. With a further increase in $CuCl_2$ loading not less than 540 ppm of Cu and 600 ppm of Cl, the O_2 uptakes decreased obviously and O_2 almost couldn't adsorb on the catalyst surface. As shown in Fig. 7 and Table 2, the appropriate $CuCl_2$ loading of Ag-$CuCl_2$/$BaCO_3$ catalyst can decrease the desorption temperature of molecular oxygen species and increase the desorption temperature of atomic oxygen species, which is in favor of epoxidation of propylene by molecular oxygen. As shown in Table 2, PO selectivity was still low (15.5 %) over Ag-$CuCl_2$/$BaCO_3$ catalyst with 180 ppm of Cu and 200 ppm of Cl, although there were molecular oxygen species adsorbed on the catalyst surface shown in Fig. 7. As shown in Fig. 7, a strong desorption peak of atomic oxygen species was observed over this catalyst with the same intensity as Ag/$BaCO_3$ catalyst, which indicated that propylene preferred to react with atomic oxygen species to produce a large amount of CO_2 and PO formation was low leading to low PO selectivity. When Ag/$BaCO_3$ catalyst was modified with 360 ppm of Cu and 400 ppm of Cl, the intensity of the desorption peak of atomic oxygen species decreased significantly, thus propylene tended to react with molecular oxygen species to produce a large quantity of PO leading to high PO selectivity. An increase in $CuCl_2$ loading greatly suppresses the dissociative adsorption of oxygen on the catalyst surface. Herein, molecular oxygen species are necessary but not sufficient for high PO selectivity. Less dissociative adsorption of oxygen is also required. High PO selectivity needs the balance between electrophilic and nucleophilic oxygen species, that is to say, molecular oxygen species and atomic oxygen species respectively in this work, which is also thought to be related to an increase in EO selectivity [26].

Fig. 8 shows O_2-TPD profiles of Ag-MCl_x/$BaCO_3$ catalysts. A very interesting phenomenon was observed that molecular oxygen species disappeared only with the coexistence of atomic oxygen species and subsurface oxygen species and desorption of atomic oxygen species shifted to lower temperature over all Ag-MCl_x/$BaCO_3$ catalysts except for Ag-$CuCl_2$/$BaCO_3$ catalyst. Combined with the catalytic performance of epoxidation of propylene by molecular oxygen over Ag-MCl_x/$BaCO_3$ catalysts shown in Table 1, only modification of $CuCl_2$ enhanced PO selectivity compared with Ag/$BaCO_3$ catalyst, which indicated that PO selectivity was higher over Ag-based catalysts with molecular oxygen species adsorbed on the catalyst surface and molecular oxygen species were the active oxygen species reacting with propylene to produce PO and atomic oxygen species were the active oxygen species reacting with propylene to produce CO_2.

Table 4 shows the catalytic performance of epoxidation of propylene by molecular oxygen over Ag/$BaCO_3$ catalysts modified with Cu, Cl or $CuCl_2$, Ag/$BaCO_3$ catalyst and $CuCl_2$/$BaCO_3$ catalyst. Compared with Ag/$BaCO_3$ catalyst, over both Ag-Cu/$BaCO_3$ and Ag-Cl/$BaCO_3$ catalysts, propylene conversion and PO selectivity decreased significantly, which indicated that the modification of only Cu or Cl couldn't improve PO selectivity except for the cooperative modification of Cu and Cl. Fig. 9 shows O_2-TPD profiles of Ag/$BaCO_3$ catalysts modified with Cu, Cl or $CuCl_2$, Ag/$BaCO_3$ catalyst and $CuCl_2$/$BaCO_3$ catalyst. The O_2 uptakes over $CuCl_2$/$BaCO_3$ catalyst were small, which indicated oxygen was difficult to adsorb on the catalyst surface and thus accounted for low propylene conversion. Molecular oxygen species were difficult to adsorb on the surface of both Ag-Cu/$BaCO_3$ and Ag-Cl/$BaCO_3$ catalysts, and molecular oxygen species could adsorb on the surface of Ag-$CuCl_2$/$BaCO_3$ catalyst with the cooperative modification of Cu and Cl. Therefore the adsorption of molecular oxygen species on the catalyst surface is necessary for achieving high PO selectivity and molecular oxygen species are the active oxygen species for PO formation.

<H3>3.5.4. C_3H_6-TPSR

To investigate the reactivity of molecular oxygen species and atomic oxygen species with propylene, C_3H_6-TPSR experiments were performed. Fig. 10 shows the products formed during C_3H_6-TPSR experiments over Ag-$CuCl_2$/$BaCO_3$ catalysts with different $CuCl_2$ loadings. The main products are PO (m/e = 58) and CO_2 (m/e = 44) detected by mass spectrometer. As shown in Fig. 10A, there were a weak peak of PO at ~80 ^oC over Ag-$CuCl_2$/$BaCO_3$ catalyst with 180 ppm of Cu and 200 ppm of Cl and a weak peak of PO at ~100 ^oC over Ag-$CuCl_2$/$BaCO_3$ catalyst with 540 ppm of Cu and 600 ppm of Cl, but a sharp peak of PO at ~90 ^oC over Ag-$CuCl_2$/$BaCO_3$ catalyst with 360 ppm of Cu and 400 ppm of Cl. The temperature of PO formation was below the desorption temperature of molecular oxygen species, which confirmed that PO was produced by propylene reacting with molecular oxygen species. No PO peaks were observed over Ag/$BaCO_3$ catalyst and Ag-$CuCl_2$/$BaCO_3$ catalyst with 720 ppm of Cu and 800 ppm of Cl. As for the formation of CO_2 shown in Fig. 10B, a sharp peak of CO_2 at ~70 ^oC was observed over Ag/$BaCO_3$ catalyst and this peak became weaker with increasing $CuCl_2$ loading, which indicated that the modification of $CuCl_2$ suppressed the formation of CO_2 from the deep oxidation of PO. Over Ag/$BaCO_3$ and Ag-$CuCl_2$/$BaCO_3$ catalysts, there was a broad peak of CO_2 at ~200 ^oC and the intensity of this peak was much higher than that at ~70 ^oC, which indicated that CO_2 was mainly produced by propylene reacting with atomic oxygen species. As shown in Fig. 7 and Fig. 10, the appropriate $CuCl_2$ doping of Ag-$CuCl_2$/$BaCO_3$ catalyst can decrease the desorption temperature of molecular oxygen species in favor of PO formation, and increase the desorption temperature of atomic oxygen species in favor of depressing combustion of propylene and deep oxidation of PO, which benefits epoxidation of propylene by molecular oxygen.

<H3>3.5.5. Catalytic reaction mechanism

A schematic diagram of epoxidation of propylene by molecular oxygen over Ag-$CuCl_2$/$BaCO_3$ catalysts with different $CuCl_2$ loadings was proposed in Fig. 11. As shown in Table 3, compared with Ag/$BaCO_3$ catalyst, when 180 ppm of Cu and 200 ppm of Cl were doped into Ag-$CuCl_2$/$BaCO_3$ catalyst, the surface concentration of Ag didn't change, which implied that Cu and Cl didn't locate on the surface of Ag nanoparticles but on the surface of $BaCO_3$ support. Taking into account O_2-TPD profiles shown in Fig. 7, molecular oxygen species became more active and atomic oxygen species almost didn't change compared with Ag/$BaCO_3$ catalyst, we could infer that there was an interaction at the interface between $CuCl_2$ and Ag located on the surface of $BaCO_3$ support. Meanwhile, oxygen was adsorbed directly on the surface of Ag at the interface in close contact with $CuCl_2$ to form more active molecular oxygen species, and oxygen was adsorbed on the surface of Ag nanoparticles and then dissociated to form atomic oxygen species. Because no Cu or Cl was located on the surface of Ag nanoparticles, the adsorption of atomic oxygen species didn't reduce leading to low PO selectivity over Ag-$CuCl_2$/$BaCO_3$ catalyst with the modification of 180 ppm of Cu and 200 ppm of Cl. When 360 ppm of Cu and 400 ppm of Cl were doped, the surface concentration of Ag decreased, which indicated that some $CuCl_2$ were located on the surface of Ag nanoparticles and depressed the dissociation adsorption of oxygen, and thus molecular oxygen species almost maintained leading to higher PO selectivity. When more $CuCl_2$ were doped, more and more surface of Ag nanoparticles and $BaCO_3$ support was covered with $CuCl_2$, then was difficult to adsorb oxygen to produce molecular oxygen species and atomic oxygen species, which resulted in lower propylene conversion and PO selectivity. Molecular oxygen species adsorbed at the interface between Ag nanoparticles and $BaCO_3$ support are responsible for PO formation, which probably can explain the size effect of Ag nanoparticles over Ag/$BaCO_3$ catalyst for epoxidation of propylene by molecular oxygen [43]. Therefore the positive effects of the appropriate modification of $CuCl_2$ are twofold to improve PO selectivity: some parts of CuCl$_2$ make adsorbed molecular oxygen species more active to produce PO easily, and other parts of CuCl$_2$ depress the dissociation adsorption of oxygen to atomic oxygen species leading to combustion of propylene to CO$_2$.

<H2>3.6. Stability of Ag-CuCl$_2$/BaCO$_3$ catalysts

Fig. 12 shows the stability of Ag-CuCl$_2$/BaCO$_3$ catalysts and CuCl$_2$/BaCO$_3$ catalysts with different CuCl$_2$ loadings. Over the four CuCl$_2$/BaCO$_3$ catalysts, PO selectivity kept nearly constant, although propylene conversion increased to a maximum at time on stream of 50 h and then decreased gradually with an increase in time on stream. Among the four Ag-CuCl$_2$/BaCO$_3$ catalysts, Ag-CuCl$_2$/BaCO$_3$ catalyst with 360 ppm of Cu and 400 ppm of Cl exhibited the best initial catalytic performance with propylene conversion of 1.3 % and PO selectivity of 71.2 %, however, with increasing time on stream, PO selectivity decreased rapidly from 71.2 % to 17.4 % at the first 200 min and then retained almost stable from 200 min to 500 min, meanwhile, propylene conversion increased slowly. PO selectivity was 13.9 % at propylene conversion of 3.2 % after reaction for 500 min over Ag-CuCl$_2$/BaCO$_3$ catalyst with 360 ppm of Cu and 400 ppm of Cl. Over Ag-CuCl$_2$/BaCO$_3$ catalysts with higher CuCl$_2$ loadings, the changing trend of PO selectivity was similar to that of Ag-CuCl$_2$/BaCO$_3$ catalyst with 360 ppm of Cu and 400 ppm of Cl, in which PO selectivity decreased significantly to nearly 15 % and propylene conversion decreased to almost zero. Interestingly, Ag-CuCl$_2$/BaCO$_3$ catalyst with 180 ppm of Cu and 200 ppm of Cl maintained both propylene conversion and PO selectivity, although the initial catalytic performance was low, in which PO selectivity was about 14 % at propylene conversion of about 4 %. This catalyst showed a good stability but was not efficient for epoxidation of propylene by molecular oxygen.

<H2>3.7. Deactivation of Ag-CuCl$_2$/BaCO$_3$ catalyst

<H3>3.7.1. Deactivation of the catalyst

Considering that Ag-$CuCl_2$/$BaCO_3$ catalyst with 360 ppm of Cu and 400 ppm of Cl had the best initial catalytic performance and the deactivation trends of Ag-$CuCl_2$/$BaCO_3$ catalyst with higher $CuCl_2$ loadings were similar, the deactivation of Ag-$CuCl_2$/$BaCO_3$ catalyst with 360 ppm of Cu and 400 ppm of Cl after reaction for 500 min was mainly studied. The main reasons of deactivation are poisoning, fouling, thermal degradation (sintering or evaporation) initiated by the high temperature, mechanical damage and leaching [59]. Table 5 compares the catalytic performance and physico-chemical properties of the fresh and the deactivated Ag-$CuCl_2$/$BaCO_3$ catalysts. As shown in Table 5, Ag and Cu contents of the fresh and deactivated catalysts determined by ICP-AES didn't change and were 4.3 wt. % and 350 ppm, respectively, which indicated that the catalyst didn't lose the active components in the course of the deactivation. Epoxidation of propylene by molecular oxygen over Ag-based catalyst is a size-dependent reaction and the particle size of Ag nanoparticles has an effect on the catalytic performance [29, 60-61]. The results show that Ag nanoparticles didn't grow up during the deactivation procedure, namely, 23.6 nm after reaction for 500 min compared with 23.1 nm of the fresh catalyst, which indicated that Ag nanoparticles existed stable on $BaCO_3$ support and the aggregation didn't happen. As shown in Fig. S3, no obvious changes were observed from TEM images of the fresh and the deactivated catalysts.

To investigate whether the reactants and the products had a negative effect on Ag-$CuCl_2$/$BaCO_3$ catalyst, the catalytic performance of the fresh catalyst pretreated with reactants and products independently at 200 ^{o}C was evaluated and shown in Table 6. As shown in Table 6, the catalytic performance of Ag-$CuCl_2$/$BaCO_3$ catalyst after the pretreatments almost didn't become worse, which indicated that the reactants and the products had little effect on the catalyst except for the pretreatment with PO-N_2. Both propylene conversion and PO selectivity decreased a little after the pretreatment with PO-N_2 for 0.5 h, more obviously after the pretreatment for 2 h. PO was thought to adsorb easily and irreversibly on the surface of

Au-based catalysts which led to the worse catalytic performance [62-63]. However, PO selectivity of 62.1 % after the pretreatment with PO-N_2 for 2 h was much higher than PO selectivity of 22.0 % after reaction for 2 h shown in Fig. 12B, which indicated that PO adsorption might not be the main reason for the catalyst deactivation and there should be another important factor responsible for the catalyst deactivation.

<H3>3.7.2. Surface composition of the catalyst

The heterogeneous catalysis is a reaction which occurs on the catalyst surface and the surface properties of the catalyst are responsible for the catalytic performance. The changes of the catalyst surface between the fresh and deactivated Ag-$CuCl_2$/$BaCO_3$ catalysts were investigated by XPS shown in Fig. S4. The binding energies of Ag, Cl and Cu elements almost didn't change after reaction for 500 min, which indicated that both the valence states of the three elements and the interaction between the three elements didn't change. However, the peak intensities of Cu 2p (Fig. S4A) and Cl 2p (Fig. S4B) of the deactivated catalyst declined remarkably compared with the fresh catalyst. The surface contents of Cu and Cl of the deactivated catalyst shown in Table 7 were 0.8 atom % and 0.5 atom % respectively, much less than those of the fresh catalyst with 2.1 atom % and 0.9 atom %. The surface content of Ag decreased a little from 10.2 atom % to 9.2 atom %. The ratio of Ag to Cu increased remarkably from 4.8 to 11.5. All these results indicate that parts of the catalyst surface are coated with coverings and coke deposition is formed during the epoxidation reaction, which probably accounts for the catalyst deactivation.

<H3>3.7.3. Coke deposition

O_2-TPO experiment is performed to demonstrate whether coke deposition is formed during the reaction. Fig. 13 shows O_2-TPO profiles of the deactivated Ag-$CuCl_2$/$BaCO_3$ catalysts with different $CuCl_2$ loadings. As shown in Fig. 13, CO_2 and H_2O were produced and O_2 was consumed over all the four catalysts, which indicated that coke deposition was formed on the surface of all the four catalysts during the epoxidation reaction. Coke deposition covers the active sites, which results in the worse catalytic performance and then the catalyst deactivation. Coke deposition is usually considered as a common reason for the catalyst deactivation for hydrocarbon reactions [64-66]. Interestingly, Ag-$CuCl_2/BaCO_3$ catalyst with 180 ppm of Cu and 200 ppm of Cl had a good stability shown in Fig. 12A, although there was also coke deposition formed during the epoxidation reaction. Maybe these active sites covered with coke deposition didn't participate in the epoxidation reaction, so the catalytic performance didn't become worse even if the active sites were covered with coke deposition. Over other three catalysts, coke deposition covered the active sites responsible for PO formation, which resulted in a significant decrease in PO selectivity and the deactivation of catalysts.

<H3>3.7.4. Mechanism of coke deposition

Fig. 14 shows the stability of Ag-$CuCl_2/BaCO_3$ catalyst with 360 ppm of Cu and 400 ppm of Cl after increasing the oxygen concentration in the feed gas. As shown in Fig. 14, unfortunately, the catalyst stability was not improved, and PO selectivity still decreased rapidly and propylene conversion increased slightly with an increase in time on stream, which indicated that the catalyst deactivation still occurred and more oxygen in the feed gas couldn't make the complete combustion of coke deposition even with increasing the molar ratio of C_3H_6 to O_2 to 1:4.5 (the molar ratio of the complete combustion of C_3H_6 to CO_2 and H_2O). Therefore changing reaction conditions can't improve the catalyst stability and coke deposition is formed intrinsically during the epoxidation reaction, that is to say, the oxygen-containing intermediates cover the active sites, which leads to the formation of coke deposition and then the catalyst deactivation.

As shown in Fig. 12B, Ag-$CuCl_2/BaCO_3$ catalyst with 360 ppm of Cu and 400 ppm of Cl deactivated rapidly with an increase in time on stream, whereas both Ag-$Cu/BaCO_3$ with 360 ppm of Cu and Ag-Cl/$BaCO_3$ with 400 ppm of Cl catalysts exhibited a good stability in spite of the bad catalytic performance shown in Fig. S5. As shown in Fig. S6, compared with the deactivated Ag-$CuCl_2$/$BaCO_3$ catalyst, the peak intensities of CO_2 and H_2O of Ag-Cu/$BaCO_3$ and Ag-Cl/$BaCO_3$ catalysts were so weak that little coke deposition was formed on the surface of Ag-Cu/$BaCO_3$ and Ag-Cl/$BaCO_3$ catalysts during the epoxidation reaction. As shown in Fig. 9, molecular oxygen species were difficult to adsorb on the surface of both Ag-Cu/$BaCO_3$ and Ag-Cl/$BaCO_3$ catalysts, and molecular oxygen species could adsorb on the surface of Ag-$CuCl_2$/$BaCO_3$ catalyst. An oxygen atom of molecular oxygen species reacts with propylene to form a PO molecule and the left oxygen atom would like to react with propylene to form CO_2 and H_2O with the molar ratio of O_2 to C_3H_6 of 4.5. Insufficient oxygen atoms react with propylene to form oxygen-containing intermediates, which can’t desorb easily and cover the active sites, and thus result in the catalyst deactivation. Over Ag-Cu/$BaCO_3$ and Ag-Cl/$BaCO_3$ catalysts without molecular oxygen species adsorbed, there were no coke deposition and catalyst deactivation. As shown in Fig. 13A, the coke deposition was observed on the surface of Ag-$CuCl_2$/$BaCO_3$ catalyst with 180 ppm of Cu and 200 ppm of Cl, however, this catalyst exhibited a good stability shown in Fig. 12A. As shown in Fig. 7, over Ag-$CuCl_2$/$BaCO_3$ catalyst with 180 ppm of Cu and 200 ppm of Cl, a large quantity of adsorbed atomic oxygen species reacted with propylene to produce CO_2 and molecular oxygen species in comparison were so few that the coverage of the active sites of molecular oxygen species adsorbed by coke deposition didn’t affect the catalytic performance. However, over Ag-$CuCl_2$/$BaCO_3$ catalysts with higher $CuCl_2$ loadings, when the amount of atomic oxygen species adsorbed decreased and molecular oxygen species played an important role for PO formation, the coverage of the active sites of molecular oxygen species adsorbed by coke deposition would result in the catalyst deactivation.

Herein, the existence of molecular oxygen species and the balance between molecular oxygen species and atomic oxygen species are necessary for achieving high PO selectivity. However, these conditions will result in the coke deposition and then the catalyst deactivation. Therefore, over Ag-$CuCl_2$/$BaCO_3$ catalyst, high PO selectivity and good catalytic stability are conflicting and the deactivation of Ag-$CuCl_2$/$BaCO_3$ catalyst with high PO selectivity seems to be inevitable.

<H2>3.8. Regeneration of Ag-$CuCl_2$/$BaCO_3$ catalyst

The catalyst deactivation was caused by the coverage of active sites by oxygen-containing intermediates produced during the epoxidation reaction, which was probably reversible. Table 8 shows the catalytic performance of the regenerated Ag-$CuCl_2$/$BaCO_3$ catalyst with 360 ppm of Cu and 400 ppm of Cl under different regeneration conditions. When the deactivated catalyst was directly impregnated with Cl or Cu or Cl and Cu (Entry 3, 4, 5, 6), the catalytic performance didn’t recover because propylene conversion became lower than that of the fresh catalyst although PO selectivity increased greatly. The removal of coke deposition by the combustion method is thought to be an easier method to recover the catalytic performance, which is usually used for a deactivated catalyst with coke deposition to restore the activity [59]. So the deactivated Ag-$CuCl_2$/$BaCO_3$ catalyst was regenerated in the quartz reactor under a gas flow of O_2-N_2 (10 vol. %) of 20 mL·min^{-1} at 200 ºC for 30 min, after which the surface contents of Ag, Cu and Cl of the regenerated catalyst were 11.4 atom %, 2.1 atom % and 0.4 atom %, respectively, determined by XPS. Compared with the fresh catalyst, the surface contents of Ag and Cu of the regenerated catalyst was almost the same except for lower surface content of Cl. Unfortunately, PO selectivity of the regenerated catalyst was still low of 15.5 % (Entry 7) probably due to loss of Cl during the combustion of coke deposition. So the deactivated catalyst was impregnated with Cl after the combustion of coke deposition, and when 200 ppm of Cl was supplemented, both propylene conversion and PO selectivity of the regenerated catalyst were the same as the catalytic performance of the fresh catalyst (Entry 9). Therefore the deactivated Ag-$CuCl_2$/$BaCO_3$ catalyst can be completely regenerated by combustion of coke deposition and then impregnation with appropriate amount of Cl.

<H1>4. Conclusions

Among Ag-MCl_x/$BaCO_3$ catalysts with different chloride promoters, Ag-$CuCl_2$/$BaCO_3$ catalyst with 360 ppm of Cu and 400 ppm of Cl, prepared by the reduction-deposition-impregnation method, exhibits the best catalytic performance for gas-phase epoxidation of propylene by molecular oxygen due to the significant synergistic effect between Ag and $CuCl_2$, in which PO selectivity of 71.2 % and propylene conversion of 1.3 % are achieved under the reaction conditions of 20 % C_3H_6 -10 % O_2-70 % N_2, 200 °C, 0.1 MPa, 3000 h^{-1}. The catalytic reaction mechanism of epoxidation of propylene by molecular oxygen over Ag-$CuCl_2$/$BaCO_3$ catalyst follows Rideal-Eley mechanism, in which propylene in the gas phase reacts with molecular oxygen species adsorbed on the surface of Ag at the interface in close contact with $CuCl_2$ to produce PO and with atomic oxygen species adsorbed on the surface of Ag nanoparticles to produce CO_2 and H_2O. The appropriate $CuCl_2$ doping of Ag-$CuCl_2$/$BaCO_3$ catalyst can make adsorbed molecular oxygen species more active to produce PO easily, meanwhile, depress the dissociation adsorption of oxygen to atomic oxygen species leading to combustion of propylene to CO_2, which benefits epoxidation of propylene by molecular oxygen. Over Ag-$CuCl_2$/$BaCO_3$ catalyst with 360 ppm of Cu and 400 ppm of Cl, only PO selectivity of 13.9 % is obtained at propylene conversion of 3.2 % after reaction for 500 min. One oxygen atom of molecular oxygen species reacts with propylene to form a PO molecule and the left insufficient oxygen atoms react with propylene to produce oxygen-containing intermediates and then to form the coke deposition which covers the active sites and thus results in the catalyst deactivation. The deactivation of Ag-$CuCl_2$/$BaCO_3$ catalyst with high PO selectivity seems to be inevitable. The deactivated Ag-$CuCl_2$/$BaCO_3$ catalyst can be completely regenerated by combustion of coke deposition and then impregnation with appropriate amount of Cl due to loss of Cl during combustion of coke deposition.

Appendix A. Supplementary Material
Supplementary material associated with this article can be found in the online version.

Acknowledgments

This work was supported by National Basic Research Program of China (2013CB933200) and Commission of Science and Technology of Shanghai Municipality (15DZ1205305).

<REF>References

<BIBL>
[1] T.A. Nijhuis, M. Makkee, J.A. Moulijn, B.M. Weckhuysen,;1; Ind. Eng. Chem. Res. 45 (2006) 3447-3459.
[2] G. Blanco-Brieva, M.C. Capel-Sánchez, M.P. Frutos, A. Padilla-Polo, J.M. Campos-Martín, J.L.G. Fierro,;1; Ind. Eng. Chem. Res. 47 (2008) 8011-8015.
[3] M. Okumura, T. Fujitani, J. Huang, T. Ishida,;1; ACS Catal. 5 (2015) 4699-4707.
[4] T. Hayashi, K. Tanaka, M. Haruta,;1; J. Catal. 178 (1998) 566-575.
[5] J. Chou, E.W. McFarland,;1; Chem. Commun. 14 (2004) 1648-1649.
[6] J.Q. Lu, X.M. Zhang, J.J. Bravo-Suárez, K.K. Bando, T. Fujitani, S.T. Oyama,;1; J. Catal. 250 (2007) 350-359.
[7] W.S. Lee, R. Zhang, M.C. Akatay, C.D. Baertsch, E.A. Stach, F.H. Ribeiro, W.N. Delgass,;1; ACS Catal. 1 (2011) 1327-1330.
[8] C.H. Liu, Y.J. Guan, E.J.M. Hensen, J.F. Lee, C.M. Yang,;1; J. Catal. 282 (2011) 94-102.
[9] B. Chowdhury, K.K. Bando, J.J. Bravo-Suárez, S. Tsubota, M. Haruta,;1; J. Mol. Catal. A: Chem. 359 (2012) 21-27.
[10] W.S. Lee, M.C. Akatay, E.A. Stach, F.H. Ribeiro, W.N. Delgass,;1; J. Catal. 313 (2014) 104-112.
[11] X. Feng, X.Z. Duan, H.Y. Cheng, G. Qian, D. Chen, W.K. Yuan, X.G. Zhou,;1; J. Catal. 325 (2015) 128-135.
[12] A. Chongterdtoonskul, J.W. Schwank, S. Chavadej,;1; J. Mol. Catal. A: Chem. 372 (2013) 175-182.
[13] X.L. Jing, H.X. Wang, H.M. Chen, J.L. Huang, D.H. Sun, Q.B. Li,;1; RSC Adv. 4 (2014) 27597-27603.
[14] W. Diao, C.D. DiGiulio, M.T. Schaal, S. Ma, J.R. Monnier,;1; J. Catal. 322 (2015) 14-23.
[15] A. Palermo, A. Husain, M.S. Tikhov, R.M. Lambert,;1; J. Catal. 207 (2002) 331-340.
[16] J.Q. Lu, J.J. Bravo-Suárez, A. Takahashi, M. Haruta, S.T. Oysma,;1; J. Catal. 232 (2005) 85-95.
[17] J.Q. Lu, J.J. Bravo-Suárez, M. Haruta, S.T. Oyama,;1; Appl. Catal. A: Gen. 302 (2006) 283-295.
[18] S. Vajda, S. Lee, K. Sell, I. Barke, A. Kleibert, V.V. Oeynhausen, K. Meiwes-Broer, A.F. Rodríguez, J.W. Elam, M.M. Pellin, B. Lee, S. Seifert, R.E. Winans,;1; J. Chem. Phys. 131 (2009) 121104.
[19] F.W. Zemichael, A. Palermo, M.S. Tikhov, R.M. Lambert,;1; Catal. Lett. 80 (2002) 93-98.
[20] G.J. Jin, G.Z. Lu, Y.L. Guo, Y. Guo, J.S. Wang, W.Y. Kong, X.H. Liu,;1; J. Mol. Catal. A: Chem. 93-95 (2004) 173-182.

[21] W. Yao, G.Z. Lu, Y.L. Guo, Y. Guo, Y.Q. Wang, Z.G. Zhang,;1; J. Mol. Catal. A: Chem. 276 (2007) 162-167.

[22] X. Zheng, Q. Zhang, Y.L. Guo, W.C. Zhan, Y. Guo, Y.S. Wang, G.Z. Lu,;1; J. Mol. Catal. A: Chem. 357 (2012) 106-111.

[23] X. Zheng, Y.L. Guo, Y. Guo, Q. Zhang, X.H. Liu, L. Wang, W.C. Zhan, G.Z. Lu,;1; Rare Metals 34 (2015) 477-490.

[24] J.T. Jankowiak, M.A. Barteau,;1; J. Catal. 236 (2005) 379-386.

[25] M.O. Ozbek, I. Onal, R.A.V. Santen,;1; ChemCatChem 5 (2013) 443-451.

[26] T.C.R. Rocha, M. Hävecker, A. Knop-Gericke, R. Schlögl,;1; J. Catal. 312 (2014) 12-16.

[27] W. Yao, X. Zheng, Y.L. Guo, W.C. Zhan, Y. Guo, G.Z. Lu,;1; J. Mol. Catal. A: Chem. 342-343 (2011) 30-34.

[28] G.Z. Lu, X.B. Zuo,;1; Catal. Lett. 58 (1999) 67-70.

[29] J.Q. Lu, M.F. Luo, H. Lei, C. Li,;1; Appl. Catal. A: Gen. 237 (2002) 11-19.

[30] J.T. Jankowiak, M.A. Barteau,;1; J. Catal. 236 (2005) 379-386.

[31] M.F. Luo, J.Q. Lu, C. Li,;1; Catal. Lett. 86 (2003) 43-49.

[32] J.R. Monnier, J.L. Stavinoha, G.W. Hartley,;1; J. Catal. 226 (2004) 321-333.

[33] R.M. Lambert, R.L. Cropley, A. Husain, M.S. Tikhov,;1; Chem. Commun. 10 (2003) 1184-1185.

[34] R.L. Cropley, F.J. Williams, O.P.H. Vaughan, A.J. Urquhart, M.S. Tikhov, R.M. Lambert,;1; Surf. Sci. 578 (2005) 85-88.

[35] D. Torres, N. Lopez, F. Illas, R.M. Lambert,;1; J. Am. Chem. Soc. 127 (2005) 10774-10775.

[36] D. Torres, N. Lopez, F. Illas, R.M. Lambert,;1; Angew. Chem. 119 (2007) 2101-2104.

[37] L.J. Yang, J.L. He, Q.H. Zhang, Y. Wang,;1; J. Catal. 276 (2010) 76-84.

[38] A. Seubsai, B. Zohour, D. Noon, S. Senkan,;1; ChemCatChem 6 (2014) 1215-1219.

[39] A. Seubsai, M. Kahn, B. Zohour, D. Noon, M. Charoenpanich, S. Senkan,;1; Ind. Eng. Chem. Res. 54 (2015) 2638-2645.

[40] W.G. Su, S.G. Wang, P.L. Ying, Z.C. Feng, C. Li,;1; J. Catal. 268 (2009) 165-174.

[41] J.L. He, Q.G. Zhai, Q.H. Zhang, W.P. Deng, Y. Wang,;1; J. Catal. 299 (2013) 53-66.

[42] A. Marimuthu, J.W. Zhang, S. Linic,;1; Science 339 (2013) 1590-1593.

[43] Q. Zhang, Y.L. Guo, W.C. Zhan, Y. Guo, L. Wang, Y.S. Wang, G.Z. Lu,;1; Catal. Today http://dx.doi.org/10.1016/j.cattod.2016.01.015.

[44] J.K. Plischke, M.A. Vannice,;1; Appli. Catal. 42 (1988) 255-283.

[45] J.Q. Lu, M.F. Luo, C. Li,;1; React. Kinet. Catal. Lett. 86 (2005) 219-224.

[46] S. Ghosh, S.S. Acharyya, R. Tiwari, B. Sarkar, R.K. Singha, C. Pendem, T. Sasaki, R. Bal,;1; ACS Catal. 4 (2014) 2169-2174.

[47] L. Ma, D.S. Wang, J.H. Li, B.Y. Bai, L.X. Fu, Y.D. Li,;1; Appl. Catal. B: Environ. 148-149 (2014) 36-43.

[48] F. Gunnarsson, H. Kannisto, M. Skoglundh, H. Härelind,;1; Appl. Catal. B: Environ. 152-153 (2014) 218-225.

[49] K. Kershen, H. Celio, I. Lee, J.M. White,;1; Langmuir 17 (2001) 323-328.

[50] C. T. Campbell,;1; Surf. Sci. 157 (1985) 43-60.

[51] M. Dean, M. Bowker,;1; J. Catal. 115 (1989) 138-147.

[52] G.W. Busser, O. Hinrichsen, M. Muhler,;1; Catal. Lett. 79 (2002) 49-54.

[53] G.I.N. Waterhouse, G.A. Bowmaker, J.B. Metson,;1; Appl. Surf. Sci. 214 (2003) 36-51.

[54] K. Yamazaki, T. Kayama, F. Dong, H. Shinjoh,;1; J. Catal. 282 (2011) 289-298.

[55] T.E. Jones, T.C.R. Rocha, A. Knop-Gericke, C. Stampfl, R. Schlögl, S. Piccinin,;1; ACS Catal. 5 (2015) 5846-5850.

[56] J. Derouin, R.G. Farber, S.L. Heslop, D.R. Killelea,;1; Surf. Sci. 641 (2015) 1-4.

[57] V.I. Bukhtiyarov, V.V. Kaichev, E.A. Podgornov, I.P. Prosvirin,;1; Catal. Lett. 57 (1999) 233-239.

[58] L. Cheng, C. Yin, F. Mehmood, B. Liu, J. Greeley, S. Lee, B. Lee, S. Seifert, R.E. Winans, D. Teschner, R. Schlogl, S. Vajda, L.A. Curtiss,;1; ACS Catal. 4 (2014) 32-39.

[59] J.A. Moulijn, A.E. Diepen, F. Kapteijn,;1; Appl. Catal. A: Gen. 212 (2001) 3-16.

[60] Y. Lei, F. Mehmood, S. Lee, J. Greeley, B. Lee, S. Seifert, R.E. Winans, J.W. Elam, R.J. Meyer, P.C. Redfern, D. Teschner, R. Schlögl, M.J. Pellin, L.A. Curtiss, S. Vajda,;1; Science 328 (2010) 224-228.

[61] L.M. Molina, S. Lee, K. Sell, G. Barcaro, A. Fortunelli, B. Lee, S. Seifert, R.E. Winans, J.W. Elam, M.J. Pellin, I. Barke, V.V. Oeynhausen, Y. Lei, R.J. Meyer, J.A. Alonso, A.F.

Rodríguez, A. Kleibert, S. Giorgio, C.R. Henry, K.H. Meiwes-Broer, S. Vajda,;1; Catal. Today 160 (2011) 116-130.

[62] G. Mul, A. Zwijnenbyrg, B.V.D. Linden, M. Makkee, J.A. Moulijn,;1; J. Catal. 201 (2001) 128-137.

[63] T.A. Nijhuis, B.M. Weckhuysen,;1; Catal. Today 117 (2006) 84-89.

[64] N. Madaan, S. Gatla, V.N. Kalevaru, J. Radnik, B. Lücke, A. Brückner, A. Martin,;1; J. Catal. 282 (2011) 103-111.

[65] S.I. Sanchez, M.D. Moser, S.A. Bradley,;1; ACS Catal. 4 (2014) 220-228.

[66] C.Z. Wang, N.N. Sun, N. Zhao, W. Wei, Y.H. Sun, C.G. Sun, H. Liu, C.E. Snape,;1; Fuel 143 (2015) 527-535.

</BIBL>

<Figure>Fig. **1.** Effect of the reaction temperature on the catalytic performance of Ag/$BaCO_3$ catalyst (A) and Ag-$CuCl_2$/$BaCO_3$ catalyst with 360 ppm of Cu and 400 ppm of Cl (B) for epoxidation of propylene by molecular oxygen.
Reaction conditions: 0.6 g catalyst, 20 % C_3H_6 -10 % O_2-70 % N_2, 0.1 MPa, 3000 h^{-1}.

<Figure>Fig. **2.** Logarithm of the reaction rate of epoxidation of propylene versus the reciprocal of reaction temperature over Ag/$BaCO_3$ catalyst and Ag-$CuCl_2$/$BaCO_3$ catalyst with 360 ppm of Cu and 400 ppm of Cl.

<Figure>Fig. **3.** Effect of GHSV on the catalytic performance of Ag-$CuCl_2$/$BaCO_3$ catalyst with 360 ppm of Cu and 400 ppm of Cl for epoxidation of propylene by molecular oxygen.

Reaction conditions: 0.6 g catalyst, 20 % C_3H_6 -10 % O_2-70 % N_2, 200 ^{o}C, 0.1 MPa.

<Figure>Fig. **4.** Cu 2p XPS (A), Cl 2p XPS (B) and Ag 3d XPS (C) spectra of Ag-$CuCl_2$/$BaCO_3$ catalysts with different $CuCl_2$ loadings.

<Figure>Fig. **5.** Dependence of the reaction rates of epoxidation of C_3H_6 on the partial pressure of O_2 (A) or the partial pressure of C_3H_6 (B) over Ag-$CuCl_2$/$BaCO_3$ catalyst with 360 ppm of Cu and 400 ppm of Cl.

<Figure>Fig. **6.** C_3H_6-TPD profiles of $CuCl_2$/$BaCO_3$ catalyst, Ag/$BaCO_3$ catalyst and Ag-$CuCl_2$/$BaCO_3$ catalyst with 360 ppm of Cu and 400 ppm of Cl.

<Figure>Fig. **7.** O_2-TPD profiles of Ag-$CuCl_2$/$BaCO_3$ catalysts with different $CuCl_2$ loadings.

<Figure>Fig. **8.** O_2-TPD profiles of Ag-MCl_x/$BaCO_3$ catalysts.

<Figure>Fig. **9.** O_2-TPD profiles of Ag/$BaCO_3$ catalysts modified with different promoters and $CuCl_2$/$BaCO_3$ catalyst.

<Figure>Fig. **10.** C_3H_6-TPSR profiles of Ag-$CuCl_2$/$BaCO_3$ catalysts with different $CuCl_2$ loadings. The MS signals of PO (m/e = 58) (A) and CO_2 (m/e = 44) (B).

<Figure>Fig. **11.** Proposed schematic diagram of epoxidation of propylene by molecular oxygen over Ag-$CuCl_2$/$BaCO_3$ catalysts with different $CuCl_2$ loadings.

<Figure>Fig. **12.** Stabilities of Ag-$CuCl_2$/$BaCO_3$ catalysts and $CuCl_2$/$BaCO_3$ catalysts with different $CuCl_2$ loadings for epoxidation of propylene by molecular oxygen. Propylene conversion (A) and PO selectivity (B) of Ag-$CuCl_2$/$BaCO_3$ catalysts with 180 ppm of Cu and 200 ppm of Cl (■), 360 ppm of Cu and 400 ppm of Cl (●), 540 ppm of Cu and 600 ppm of Cl (▲), 720 ppm of Cu and 800 ppm of Cl (▼). Propylene conversion (A) and PO selectivity (B) of $CuCl_2$/$BaCO_3$ catalysts with 180 ppm of Cu and 200 ppm of Cl (▓□), 360 ppm of Cu and 400 ppm of Cl (◇), 540 ppm of Cu and 600 ppm of Cl (☆), 720 ppm of Cu and 800 ppm of Cl (○).

Reaction conditions: 0.6 g catalyst, 20 % C_3H_6 -10 % O_2-70 % N_2, 200 °C, 0.1 MPa, 3000 h^{-1}.

<Figure>Fig. **13.** O_2-TPO profiles of the deactivated Ag-$CuCl_2$/$BaCO_3$ catalysts with different $CuCl_2$ loadings. 180 ppm Cu of and 200 ppm of Cl (A), 360 ppm of Cu and 400 ppm of Cl (B), 540 ppm of Cu and 600 ppm of Cl (C), 720 ppm of Cu and 800 ppm of Cl (D).

<Figure>Fig. **14.** Stability of Ag-$CuCl_2$/$BaCO_3$ catalyst with 360 ppm of Cu and 400 ppm of Cl under the feed gas with different O_2 concentration.

Tables

<Table>Table 1 Effects of the chloride promoters on the catalytic performance of Ag-MCl_x/$BaCO_3$ catalysts with 400 ppm of Cl.

Chlorides	Propylene conversion (%)	Selectivity (%)		
		PO	PA	CO_2
--	12.5	36.9	--	63.1
NH_4Cl	0.3	21.5	0.8	77.7
NaCl	0.5	24.3	0.3	75.4
KCl	2.0	16.8	0.2	83.0
$CaCl_2$	0.4	24.3	0.5	75.2
$FeCl_3$	0.6	12.0	0.3	87.7
$CuCl_2$	1.3	71.2	0.2	28.6
CuCl	5.2	26.1	0.3	73.6

Reaction conditions: 0.6 g catalyst, 20 % C_3H_6 -10 % O_2-70 % N_2, 200 °C, 0.1 MPa, 3000 h^{-1}.

<Table>Table 2 Effect of $CuCl_2$ loading on the catalytic performance of $CuCl_2$/$BaCO_3$ and Ag-$CuCl_2$/$BaCO_3$ catalysts.

Reaction conditions: 0.6 g catalyst, 20 % C_3H_6 -10 % O_2-70 % N_2, 200 ^{o}C, 0.1 MPa, 3000 h^{-1}.

[a] Determined from XRD patterns shown in Fig. S1 by Scherrer's equation.

<Table>Table 3 The surface composition of Ag-$CuCl_2$/$BaCO_3$ catalysts with different $CuCl_2$ loadings.

Catalysts	Surface composition			
	Ag (atom %)	Cu (atom %)	Cl (atom %)	Ag/Cu
Ag/$BaCO_3$	12.4	--	--	--
Ag-180ppmCu-200ppmCl/$BaCO_3$	12.5	1.6	0.7	7.8
Ag-360ppmCu-400ppmCl/$BaCO_3$	10.2	2.1	0.9	4.8
Ag-540ppmCu-600ppmCl/$BaCO_3$	3.6	2.6	--	1.4
Ag-720ppmCu-800ppmCl/$BaCO_3$	2.9	2.9	--	1.0

<Table>Table 4 The catalytic performance of Ag/$BaCO_3$ catalysts modified with different promoters and $CuCl_2$/$BaCO_3$ catalyst.

Catalysts	Propylene conversion (%)	Selectivity (%)		
		PO	PA	CO_2
Ag/$BaCO_3$	12.5	36.9	--	63.1
Ag-Cu/$BaCO_3$ [a]	6.9	6.2	--	93.8
Ag-Cl/$BaCO_3$ [b]	0.3	21.5	0.8	77.7
Ag-$CuCl_2$/$BaCO_3$	1.3	71.2	0.2	28.6
$CuCl_2$/$BaCO_3$	0.1	28.1	1.9	70.0

Reaction conditions: 0.6 g catalyst, 20 % C_3H_6 -10 % O_2-70 % N_2, 200 ^{o}C, 0.1 MPa, 3000 h^{-1}.

[a] $Cu(NO_3)_2$ was used as the precursor of Cu with 360 ppm of Cu.

[b] NH_4Cl was used as the precursor of Cl with 400 ppm of Cl.

<Table>Table 5 The comparison between the fresh and deactivated Ag-$CuCl_2$/$BaCO_3$ catalysts with 360 ppm of Cu and 400 ppm of Cl after reaction for 500 min.

Catalysts	Propylene conversion (%)	Selectivity (%)			Ag content (wt. %) [a]	Cu content (ppm) [a]	Ag crystallite size (nm) [b]
		PO	PA	CO_2			
Fresh	1.3	71.2	0.2	28.6	4.3	350	23.1

Deactivated	3.2	13.9	0.1	86.0	4.3	350	23.6

Reaction conditions: 0.6 g catalyst, 20 % C_3H_6 -10 % O_2-70 % N_2, 200 °C, 0.1 MPa, 3000 h^{-1}.

[a] Measured by ICP-AES.

[b] Determined from XRD patterns by Scherrer's equation.

<Table>Table 6 The catalytic performance of Ag-$CuCl_2/BaCO_3$ catalyst with 360 ppm of Cu and 400 ppm of Cl pretreated with reactants and products independently at 200 °C.

Pretreatment atmospheres	Temperature (°C)	Time (h)	Propylene conversion (%)	Selectivity (%)		
				PO	PA	CO_2
No	--	--	1.3	71.2	0.2	28.6
20%C_3H_6-N_2	200	0.5	1.4	79.1	0.3	20.6
10%O_2-N_2	200	0.5	1.1	67.0	0.2	32.8
	200	2.0	1.1	70.6	0.3	29.1
CO_2	200	0.5	1.0	76.9	0.2	22.9
PO-N_2	200	0.5	0.9	66.5	0.2	33.3
	200	2.0	0.8	62.1	0.3	37.6
H_2O-N_2	200	0.5	1.0	68.8	0.3	30.9

Reaction conditions: 0.6 g catalyst, 20 % C_3H_6 -10 % O_2-70 % N_2, 200 °C, 0.1 MPa, 3000 h^{-1}.

<Table>Table 7 The comparison of the surface compositions of the fresh and deactivated Ag-$CuCl_2/BaCO_3$ catalysts.

Catalysts	Ag (atom %)	Cu (atom %)	Cl (atom %)	Ag/Cu
Fresh	10.2	2.1	0.9	4.8
Deactivated	9.2	0.8	0.5	11.5

<Table>Table 8 The catalytic performance of the regenerated Ag-$CuCl_2/BaCO_3$ catalyst under different regeneration conditions.

Entry	Regeneration conditions	Propylene conversion (%)	Selectivity (%)		
			PO	PA	CO_2
1	Fresh	1.3	71.2	0.2	28.6
2	Deactivated	3.2	13.9	0.1	86.0
3	D [a] +100 ppm Cl [c]	0.6	53.4	0.4	46.2
4	D + 200 ppm Cl	0.9	73.5	0.9	25.6
5	D + 180 ppm Cu [d]	0.8	51.9	0.8	47.3
6	D + 180 ppm Cu + 200 ppm Cl	0.5	70.8	2.6	26.6
7	D + CR [b]	2.5	15.5	0.3	84.2
8	D + CR + 100 ppm Cl	0.7	61.9	0.4	37.7
9	D + CR + 200 ppm Cl	1.3	75.2	0.6	24.2

Reaction conditions: 0.6 g catalyst, 20 % C_3H_6 -10 % O_2-70 % N_2, 200 °C, 0.1 MPa, 3000 h^{-1}.

[a] D represented deactivated.

[b] CR represented coke removal.

[c] NH_4Cl as the precursor of Cl.

[d] $Cu(NO_3)_2$ as the precursor of Cu.

TDENDOFDOCTD